Korean J. Chem. Eng., 39(1), 209-215 (2022)
DOI: 10.1007/s11814-021-0938-6

pISSN: 0256-1115
eISSN: 1975-7220

Nanocomposite design of graphene modified TiO_2 for electrochemical sensing in phenol detection

Muhammad Nurdin*,†, Maulidiyah Maulidiyah*, Abdul Haris Watoni*, Armawansa Armawansa*, La Ode Agus Salim*, Zul Arham, Dwiprayogo Wibowo***, Irwan Irwan*, and Akrajas Ali Umar******

*Department of Chemistry, Faculty of Mathematics and Natural Sciences, Universitas Halu Oleo, Kendari 93232 - Southeast Sulawesi, Indonesia
**Department of Mathematics and Natural Sciences, Institute Agama Islam Negeri (IAIN), Kendari 93563 - Southeast Sulawesi, Indonesia
***Department of Environmental Engineering, Universitas Muhammadiyah Kendari, Kendari 93127 - Southeast Sulawesi, Indonesia
****Institute of Microengineering and Nanoelectronics, Universiti Kebangsaan Malaysia, 43600 UKM Bangi, Selangor, Malaysia
(*Received 29 March 2021 • Revised 19 August 2021 • Accepted 24 August 2021*)

Abstract−This study is the stage of developing a phenol detection electrochemical sensor. Phenol is one of the organic pollutants harmful to human life and ecosystems. The development of this sensor was carried out by studying the use of TiO_2 anatase as a modifier of graphene electrodes. The mass of TiO_2 anatase was varied, while the mass of graphene and paraffin was fixed. The results showed that the TiO_2 mass of 1.0 g was the best mass as a graphene electrode modifier. The use of this mass increases the oxidation current (I_{pa}) of phenol by 450 A, which is observed at an oxidation potential (E_{pa}) of −0.30 V. The presence of interfering ions such as K^+, Fe^{2+}, and OH^- can decrease the measurement current. However, based on the %RSD value, it shows that the performance of TiO_2-graphene is in a good category, where the %RSD value obtained is 0.6%. TiO_2-graphene electrodes can be used repeatedly for 12 days. Overall, this work demonstrates the potential of TiO_2-graphene electrodes as electrode candidates for electrochemical-based phenol sensors.

Keywords: Anatase TiO_2, Electrochemical Sensor, Electrode Modifier, Graphene, Phenol

INTRODUCTION

Persistent organic pollutants (POPs) are a serious concern for environmental researchers. POPs are widely used as active ingredients in pesticides. Their presence in the environment is reported to have a negative impact on humans and ecosystems. POPs are known to be toxic, stable, persistent, and can undergo high bioaccumulation in the environment. Among the POPs derivative compounds is phenol (C_6H_5OH), which is found in many types of pesticides [1]. In the market, phenol is known by several names, such as carbolic acid, benzenol, phenylic acid, hydroxybenzene, and phenic acid. This compound is very dangerous, toxic, carcinogenic [2]. In addition, it can cause damage to the function of body organs and birth defects [3]. Its presence is declared safe for aquatic ecosystems if the concentration is 0.5-1.0 M, while the concentration for drinking water quality standards is 0.01 M [4].

The electrochemical is a method that is being developed for the detection of phenol. In general, the electrochemical method consists of several measurement techniques, one of which is the voltammetry technique. This technique is reported to have high sensitivity and selectivity, low detection limit, simple preparation, and low current interference [5]. In its development, sensitivity and selectivity are strongly influenced by the choice of working electrode [6-8]. Recent studies have shown that the use of modifiers greatly affects the performance of the electrodes. In this regard, the TiO_2 modifier has been reported to be used as a carbon paste electrode (CPE) composite. TiO_2 is effective in increasing the sensitivity of CPE in detecting compounds, such as cypermethrin [9], fipronil [10,11], and heavy metals [11]. Electrode performance is also supported by the use of electrolytes. The mechanism of electron transfer in the solution body causes a difference in the concentration of the analyte on the electrode surface with the solution body [11,12]. The presence of a supporting electrolyte will help prevent the occurrence of unwanted currents in voltammetry measurements, such as migration and convection currents [13]. Thus, the selection of electrolytes is very important to support electrochemical processes because of the resulting stability for reproducibility, high conductivity, and electrode selectivity [14].

Currently, graphene is an electrode material with good stability. It has high electron mobility (~10,000 cm^2/Vs), quantum space effects (strong magnetism and low temperature), high optical properties (97.7%), high surface area (2,630 $m^2 \cdot g^{-1}$), good conductivity, and is good at high temperatures (~3,000 W/mK) [15]. Therefore, modification of this material with TiO_2 will obtain a unique composite material that has high conductivity, stability, low cost, and is environmentally friendly [16-19]. Graphene plays a role in good elec-

†To whom correspondence should be addressed.
E-mail: mnurdin06@yahoo.com

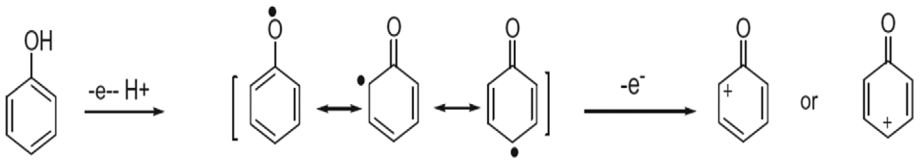

Fig. 1. Oxidation mechanism of phenol.

tron transfer because the carbon bonds provide segment holes for electrons coming from the TiO_2 material. A high sensing electrochemical sensor based on TiO_2-graphene nanocomposites was evaluated to high transfer electron, analytical sensor performance, and its utilization for sensor electrochemical.

In this study, the performance of TiO_2-graphene was studied in detecting phenol. During the electrochemical process, phenol undergoes an oxidation reaction by losing two electrons. The mechanism of phenol oxidation is shown in Fig. 1. This work is expected to be able to obtain electrodes with high electron transfer.

MATERIALS AND METHODS

1. Synthesis of Electrode Nanocomposite

TiO_2 anatase was synthesized directly using TiO_2 Degussa P25 (Merck, CAS number: 13463-67-7). In summary, 10 g of TiO_2 Degussa P25 were placed in a porcelain dish and hydrothermally annealed at 500 °C for 3 hours [20,21]. Next, TiO_2 anatase was mixed homogeneously with graphene (Sigma-Aldrich, CAS number: 763713). The homogenization process refers to the work of Tavakkoli et al. [22]. The amount of TiO_2 anatase used was 0.05 g, 0.1 g, 0.5 g, and 1.0 g, while graphene was 0.5 g. Both were put into a vial containing 0.3 g of liquid paraffin (Sigma-Aldrich, CAS number: 76235, ρ=0.88 g·cm^{-3}) and stirred for 25 minutes. The nanocomposite was then inserted into a 0.3 mm diameter glass electrode body. This electrode body was connected with Cu wire. The nanocomposite was compacted by pressing and smoothing the surface of the electrode body.

2. Characterization

The TiO_2 anatase crystalline nature was characterized using X-ray diffraction, XRD (Shimadzu 6000) at 2θ=20-80° with Cu-Kα= 1.54060. The morphology of the nanocomposites was characterized using scanning electron microscopy-energy dispersive X-ray, SEM-EDX (HITACHI SU3500). Meanwhile, the electrochemical properties of nanocomposite were characterized by cyclic voltammetry technique using a potentiostat DY2100. The probe design for voltammetric measurements can be seen in Fig. 2. Where, the probe used is a glass container (diameter: ±2.00 cm; height: ±3.50 cm). The probe has a top cover with three holes as a place for electrodes, both working, pointer and auxiliary electrodes.

3. Experimental Design of Phenol

The detection of phenol (Sigma-Aldrich, CAS number: 108-95-2) involved using a 3-electrode-based cyclic voltammetry technique as shown in Fig. 1. TiO_2-Graphene electrode was placed as the working electrode. $NaNO_3$ 1.0 M (Sigma-Aldrich, CAS number: 7631-99-4) was used as the supporting electrolyte. During the detection of phenol, the instrument potential window applied was ±0.8 V, with a scan rate of 0.1 V.

RESULTS AND DISCUSSION

1. Characterization of Nanocomposites

TiO_2 anatase synthesis method directly through hydrothermal annealing is effective in producing TiO_2 anatase with high optical density. Bakardjieva et al. [23] reported that the annealing process in the temperature range of 500-800 °C was a good condition in converting the amorphous phase to anatase. Interest in anatase is due to its optical properties and high electron transfer charge [24]. The results of XRD analysis showed that TiO_2 anatase was formed with good purity (Fig. 3). This is corroborated by the appearance of specific diffractogram peaks at 2θ=25.0° (101); 37.7° (112); 48.0° (200); 53.8° (105); 55.0° (211); 62.6° (204); and 68.0° (116). These values are specific values for TiO_2 anatase [25]. In addition,

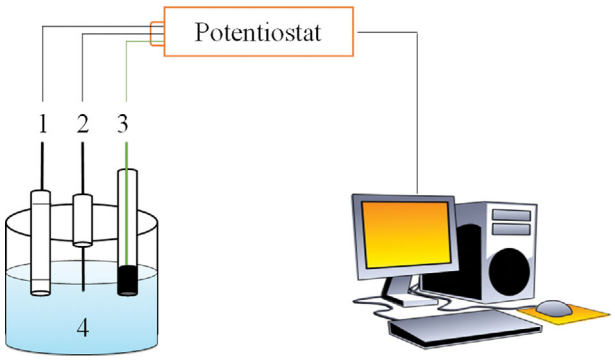

Fig. 2. Probe design to the voltammetric measurement: (1) reference electrode (Ag/AgCl), (2) auxillary electrode (Pt wire), (3) working electrode, (4) electrolyte solution.

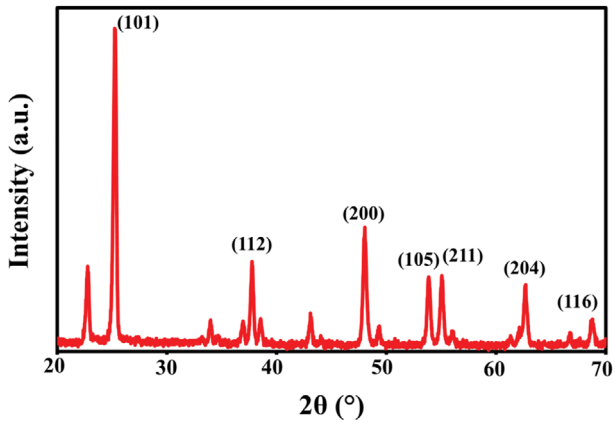

Fig. 3. XRD pattern of TiO_2 anatase by hydrothermal annealing.

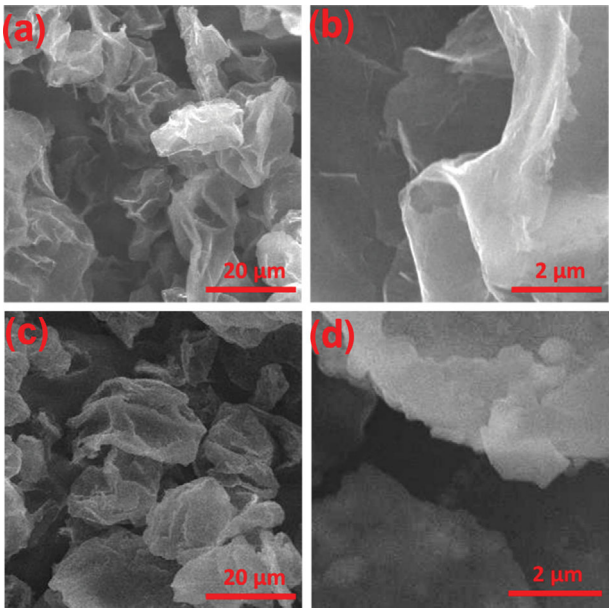

Fig. 4. SEM morphology, (a), (b) graphene nanosheets, (c), (d) TiO_2-graphene nanocomposites.

the peak in the diffractogram also explains that there is no peak for the rutile and brookite phases [9].

Fig. 4 shows the morphology of graphene nanosheets and TiO_2-graphene nanocomposites. Graphene morphology (Fig. 4(a), (b)) is composed of nano-sheets derived from graphite. This graphite contains functional groups such as -OH, -COOH which promote physical and mechanical interactions between the polymer and the nanosheet [26]. The TiO_2-graphene shows a homogeneous morphology (Fig. 4(c), (d)). Basheer [27] explained that the interaction between TiO_2 and graphene nanosheets occurs through strong chemisorption and physisorption. The graphene nanosheet appears transparent and folded on one side. This is supported by EDX

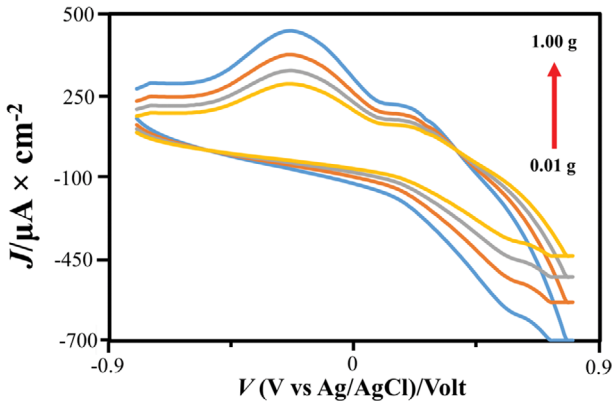

Fig. 6. Cyclic voltammogram of TiO_2 amount variation.

analysis which shows that the constituent element of the graphene nanosheet is carbon (Fig. 5(a)). While Fig. 5(b) shows the number of O atoms is more than Ti atoms. This is due to the nature of the O atom which is very easy to form C-O bonds compared to Ti-O [27]. These results strengthen the assumption that the addition of TiO_2-graphene nanocomposite produces a more homogeneous and uniform pore surface.

2. Characterization Electrochemical

2-1. Optimization of Amount of Anatase TiO_2

The amount of the TiO_2 modifier was optimized using 0.1 M phenol solution with 1.0 M $NaNO_3$ as the supporting electrolyte. The choice of $NaNO_3$ was based on its good properties in increasing electron transfer. Another consideration is that phenol does not react with $NaNO_3$. It is different if the supporting electrolyte used is acidic, such as H_2SO_4. Its use can convert phenol into 4-nitrophenol [24,25]. Electron transfer results from phenol being conjugated in a cyclic ring [30]. Fig. 6 is a cyclic voltammogram of TiO_2-graphene nanocomposite in 0.1 M phenol solution. These results show the effect of TiO_2 modifier amount in improving elec-

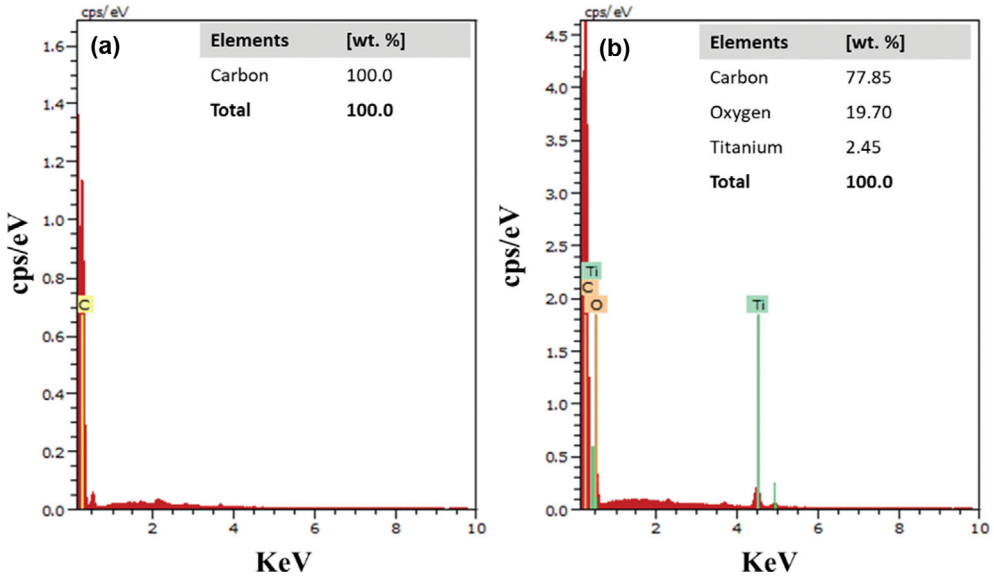

Fig. 5. EDX area analysis: (a) Graphene nanosheets, (b) TiO_2-graphene nanocomposites.

trode performance. Where, an amount of 1.0 g produces the highest anodic current (I_{pa}) of 450 A. This current occurs at an anodic potential value (E_{pa}) of −0.30 V, which is the oxidation potential of the phenol on the surface of the TiO_2-graphene electrode. In previous work, TiO_2 modifier was reported to have good stability in assisting electron transfer [17,18].

2-2. Scan Rate Variation

Scan rate variation was carried out using graphene electrodes with the addition of 1.0 g TiO_2. This composition is the best composition obtained during optimization of TiO_2 amount. The potential scan rate tested is 0.05, 0.10, 0.20 and 0.50 $V{\cdot}s^{-1}$. The linear correlation between the potential scan rate and the Ipa of phenol shows that the phenol oxidation process is controlled by the rate of diffusion. Fig. 7 shows a cyclic voltammogram of phenol oxidation at different potential scan rates. The high scan rate can be caused by the thinning of the diffusion layer on the electrode surface [26,27].

2-3. Electrode Performance Test

The electrochemical performance of TiO_2-graphene was studied in $K_3[Fe(CN)_6]$ solution by comparing it to graphene electrodes in the absence of TiO_2. $K_3[Fe(CN)_6]$ has stable redox property with a clear number of electrons [29]. The redox reaction is reversible with the following equation:

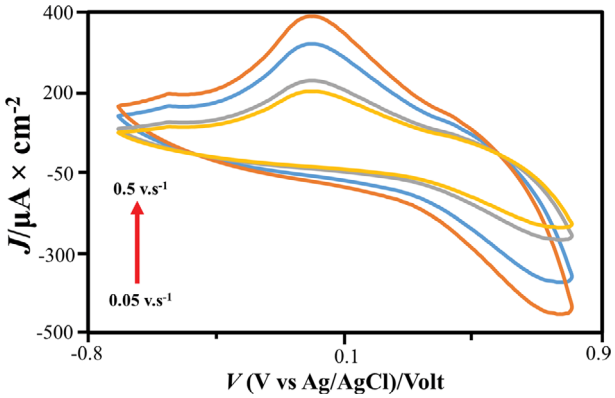

Fig. 7. Scan rate variation of TiO_2-graphene nanocomposites.

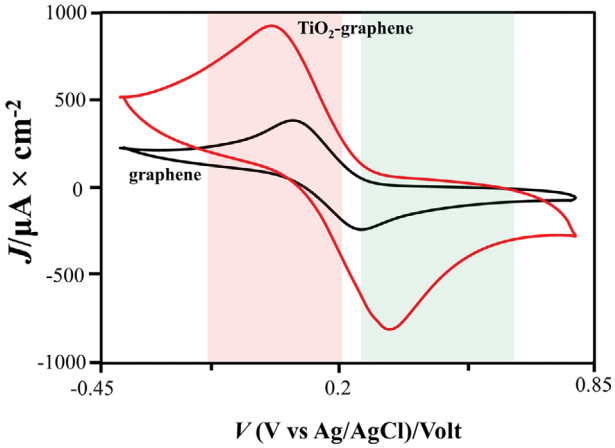

Fig. 8. Cyclic voltammogram of graphene nanosheet and TiO_2-graphene in 0.1 M $K_3[Fe(CN)_6]$.

$$Fe(CN)^{3-}_{6\ (aq)} + e^- \rightleftharpoons Fe(CN)^{4-}_{6\ (aq)} \quad (E_0 = 0.356\ V)$$

Fig. 8 is a cyclic voltammogram of graphene nanosheet (black line) and TiO_2-graphene (red line) in $K_3[Fe(CN)_6]$ solution. The high electron transfer is shown by TiO_2-graphene. This explains that there is an effect of the surface area of the nanocomposite [33]. Based on the voltammogram, TiO_2-graphene has I_{pa} and I_{pc} values of 910 A and 810 A, respectively. While the I_{pa} and I_{pc} values of graphene nanosheets are 400 A and 250 A, respectively. Based on these data, it can be concluded that TiO_2-graphene has much better performance for phenol detection.

3. Determination of Phenol Detection

3-1. Linearity and Limit of Detection

The linearity area is a linear curve that results from plots of flow and analyte concentration. In this work, the phenol concentration range used is 10^{-1} M to 10^{-6} M. In addition, the limit of detection (LoD) is also calculated to determine the smallest phenol concen-

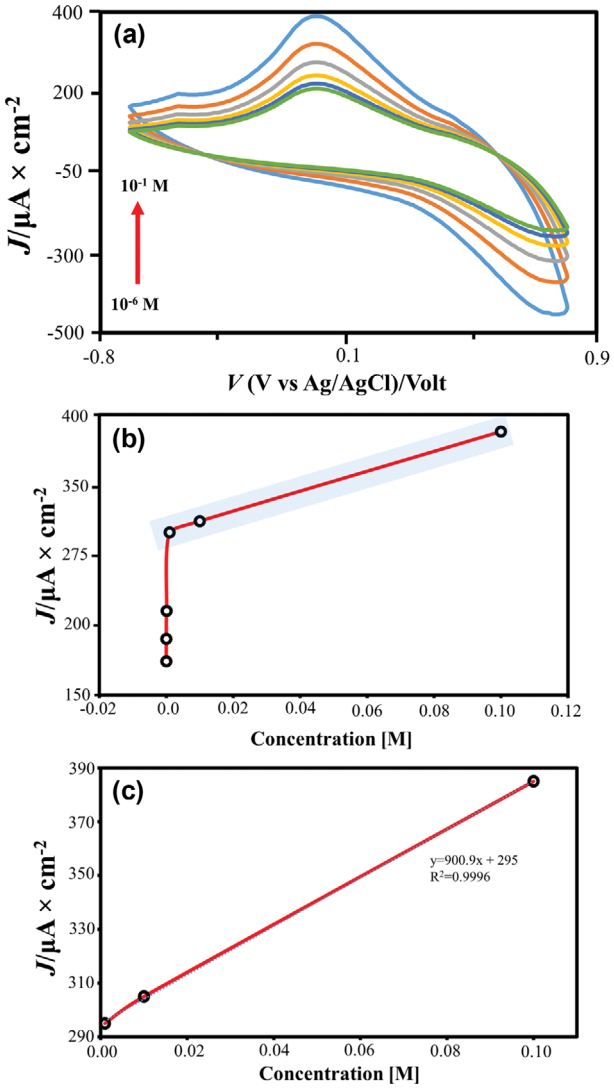

Fig. 9. Linearity and LoD of TiO_2-graphene: (a) Phenol voltammogram at concentration of 10^{-6} M-10^{-1} M, (b) Graph between phenol concentration and I_{pa} value, (c) Linearity area of phenol at concentration range of 10^{-3} M-10^{-1} M.

tration in the analyte that can still be detected and gives a significant current response. According to Bakker et al. and Bulhlmann et al., the limit of detection (LoD) is the lowest concentration of analyte that can be detected by the analytical procedure [34,35]. The results of the linearity and LoD area measurements can be seen in Fig. 9.

Fig. 8(a) shows a linear relationship between the phenol concentration and the I_{pa} value. Nurdin et al. reported that the increase in I_{pa} value was proportional to the increase in analyte concentration. In this work, the I_{pa} values obtained for each concentration were 385 A (10^{-1} M); 305 A (10^{-2} M); 295 A (10^{-3} M); 225 A (10^{-4} M); 200 A (10^{-5} M), and 180 A (10^{-6} M). Plots of phenol versus I_{pa} concentrations are shown in Figs. 8(b) and 8(c). The results show that the linearity range occurs at concentrations of 10^{-3} M to 10^{-1} M

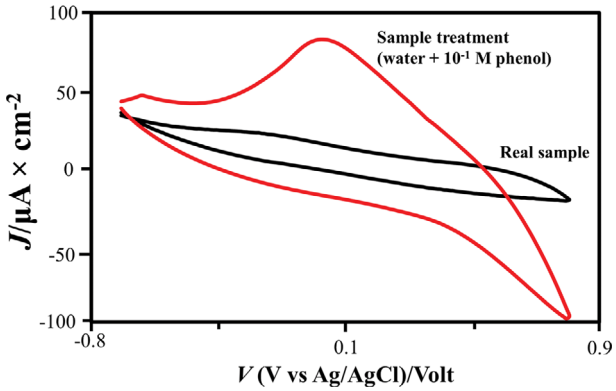

Fig. 10. Cyclic voltammogram of real sample detection.

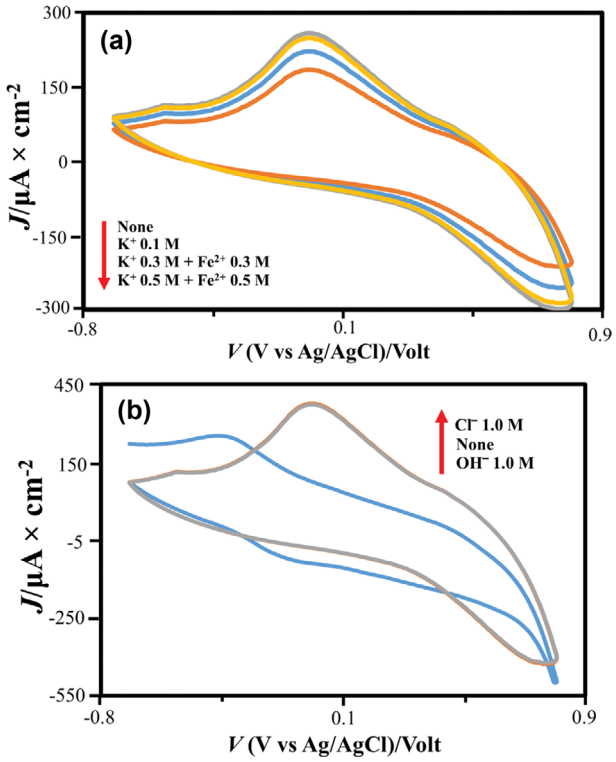

Fig. 11. Interference ions: (a) cation and (b) anion.

with a slope of 900.6, an intercept of 295, and R^2=0.9996. Based on the calculation results obtained LoD of 0.004 M.

3-2. Real Sample Detection

Determination of real samples was carried out on drinking water samples. Fig. 10 shows the performance of the TiO_2-graphene electrode in detecting phenol. Where, in drinking water samples, no phenol oxidation peak was observed (black line). This indicates that the drinking water sample does not contain phenol. Another reason is that the phenol concentration is much lower than the detection limit of TiO_2-graphene [36]. It was different when the sample was added with 0.1 M standard phenol solution (red line). The addition of the standard solution causes the appearance of a specific oxidation peak for phenol. These results indicate that TiO_2-graphene has good sensitivity in detecting phenol.

3-3. Ionic Interference Test

The ion interference test was carried out to study the effect of the ions in the solution. The presence of ions, both cations and anions in solution, is reported to affect the properties of phenol [37]. In this work, the test was carried out by adding cations such as KOH (K^+) and $Fe(OH)_2$ (Fe^{2+}). The concentration of K^+ ions tested was 0.1 M, 0.3 M, and 0.5 M, while the Fe^{2+} ions were 0.3 M and 0.5 M. Fig. 11(a) shows the effect of cations on the I_{pa} value of phenol. Where, the large number of cations causes a decrease in

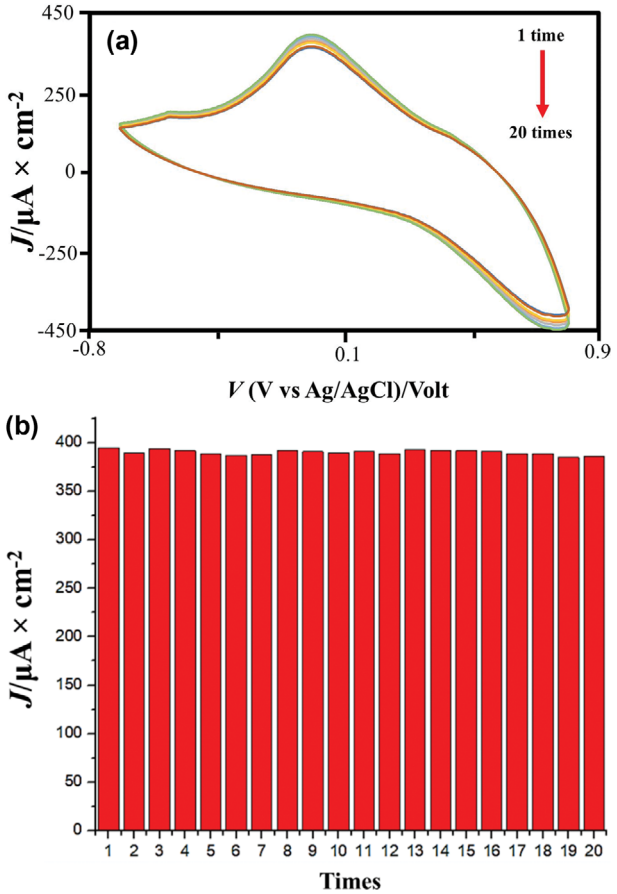

Fig. 12. Repeatability performance using TiO_2-graphene nanocomposites: (a) Voltammogram repeatability analysis, (b) measurement of accuracy repeatability.

I_{pa}. In addition, the concentration of cations also has an effect on the decrease. The decrease in I_{pa} occurs due to the increased interaction of the positive charge from the cation with the negative charge on the surface of the electrode. The interaction of these charges causes a thickening of the electrical double layer in the solution body, resulting in slower electron transfer [38]. Fig. 11(b) shows the effect of anions on the detection of phenol. The anions tested came from the addition of 1.0 M NaOH (OH^-) and 1.0 M HCl (Cl^-) in the test solution. Based on the data, the presence of OH^- causes a decrease in the peak current and a shift in the value of the oxidation potential of phenol. The shift in the oxidation value of phenol can be caused by the basic nature of NaOH [39]. In contrast to OH^- ions, the presence of Cl^- ions in the test solution increases the I_{pa} value. The resulting current is greater than without the addition of anions. The Cl^- ion is reported as an electron-carrying anion, where it contributes to the supply of electrons in the solution body [40].

3-4. Repeatability Test

Repeatability test is a technique for method precision, which can be determined by repeated testing of one electrode. The test results describe the stability of the working electrode used. In addition, standard deviation (SD) and relative standard deviation (RSD) can be calculated. Fig. 12 shows the results of the repeat test of the TiO_2-graphene electrode in a phenol solution. The test was carried out for 20 repetitions. Based on the data obtained, it is known that the SD value is 2.32 with an average peak current of 381 A. While the RSD value from this test is 0.6%. This value is determined by dividing the SD by the average peak phenol current multiplied by 100%.

3-5 Lifetime Working Electrode

The lifetime of the TiO_2-graphene electrode was tested for 30 days. This condition is to determine the resistance of the electrode during the determination of phenol. Fig. 13 shows that day 1 to day 12 of the electrode is relatively stable, while day 15 to day 30 the resulting current decreases. This phenomenon explains that saturation occurs at the electrode surface. Phenol molecules can be adsorbed on the surface of TiO_2-graphene, so the electron transfer is slow and the peak current will be reduced.

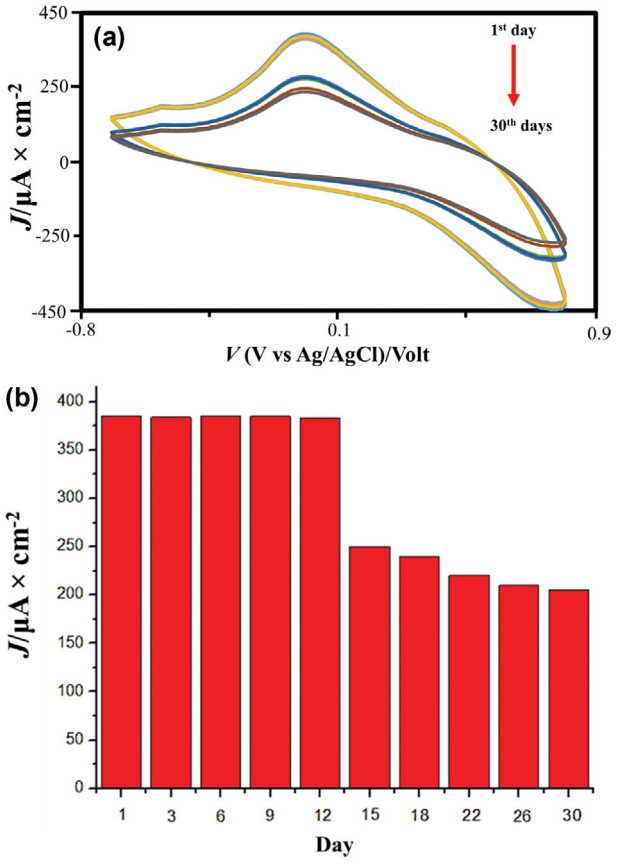

Fig. 13. Lifetime determination by using TiO_2-graphene nanocomposites: (a) Voltammogram lifetime analysis, (b) measurement of accuracy lifetime.

CONCLUSION

The performance of TiO_2-graphene nanocomposite electrodes for phenol detection has been investigated. It was found that the TiO_2-graphene nanocomposite was effective in detecting phenol in the samples based on the voltammetric technique. The TiO_2-graphene nanocomposite had high electrochemical performance with an I_{pa} value of 450 A and an E_{pa} value of −0.30 V. In addition, it is also known that the voltammetric response is influenced by the presence of cations and anions in the sample. Based on the calculation results, the LoD value is 4×10^{-3} M and the Horwitz Ratio (HorRat) value is 0.6%. Overall, this work demonstrates the potential of TiO_2-graphene electrode as one of the electrode candidates for the determination of phenol molecules in aquatic environments.

ACKNOWLEDGEMENTS

We acknowledge the financial support from the Ministry of Education and Culture of the Republic of Indonesia under the Applied Research award grant no 270/E4.1/AK.04.PT/ 2021 and Ministry of Education, Culture, Research and Technology of the Republic of Indonesia under the World Class Professor award grant no 2817/E4.1/KK.04.05/2021.

REFERENCES

1. M. Farzadkia, Y. Dadban Shahamat, S. Nasseri, A. H. Mahvi, M. Gholami and A. Shahryari, *J. Eng.*, **520929**, 1 (2014).
2. Y. D. Shahamat, M. Farzadkia, S. Nasseri, A. H. Mahvi, M. Gholami and A. Esrafili, *J. Environ. Heal. Sci. Eng.*, **12**, 1 (2014).
3. Y. Pi, X. Li, Q. Xia, J. Wu, Y. Li, J. Xiao and Z. Li, *Chem. Eng. J.*, **337**, 351 (2017).
4. S. B. Slamet, A. Rita and S. Zulaina, *J. Teknol.*, 303 (2006).
5. Y. Zhang, M. Zhang, Q. Wei, Y. Gao, L. Guo, K. A. Al-Ghanim, S. Mahboob and X. Zhang, *Sensors*, **16**, 535 (2016).
6. D. Wibowo, Ruslan, Maulidiyah and M. Nurdin, *IOP Conf. Ser. Mater. Sci. Eng.*, **267**, 012007 (2017).
7. Hikmawati, A. H. Watoni, D. Wibowo, Maulidiyah and M. Nurdin, *IOP Conf. Ser. Mater. Sci. Eng.*, **267**, 012005 (2017).
8. M. Maulidiyah, T. Azis, L. Lindayani, D. Wibowo, L. O. A. Salim,

A. Aladin and M. Nurdin, *J. Electrochem. Sci. Technol.*, **10**, 394 (2019).
9. M. Nurdin, M. Maulidiyah, L. O. A. Salim, M. Z. Muzakkar and A. A. Umar, *Microchem. J.*, **145**, 756 (2018).
10. M. Nurdin, O. A. Prabowo, Z. Arham, D. Wibowo, M. Maulidiyah, S. K. M. Saad and A. A. Umar, *Surf. Interfaces*, **16**, 108 (2019).
11. M. Nurdin, Z. Arham, J. Rasyid, M. Maulidiyah, F. Mustapa, H. Sosidi, R. Ruslan and L. O. A. Salim, *J. Phys. Conf. Ser.*, **1763**, 012067 (2021).
12. S. M. Khopkar, *Basic concepts of analytical chemistry*, New Age International (1998).
13. A. J. Bard and L. R. Faulkner, *Electrochem. Methods*, **2**, 482 (2001).
14. X. Wang, L. Zhi and K. Müllen, *Nano Lett.*, **8**, 323 (2008).
15. M. Nurdin, L. Agusu, A. A. M. Putra, M. Maulidiyah, Z. Arham, D. Wibowo, M. Z. Muzakkar and A. A. Umar, *J. Phys. Chem. Solids*, **131**, 104 (2019).
16. M. Nurdin, L. O. A. N. Ramadhan, D. Darmawati, M. Maulidiyah and D. Wibowo, *J. Coatings Technol. Res.*, **15**, 395 (2018).
17. Maulidiyah, T. Azis, A. T. Nurwahidah, D. Wibowo and M. Nurdin, *Environ. Nanotechnology, Monit. Manag.*, **8**, 103 (2017).
18. M. Nurdin, A. Zaeni, E. T. Rammang, M. Maulidiyah and D. Wibowo, *Anal. Bioanal. Electrochem.*, **9**, 480 (2017)
19. M. Natsir, Y. I. Putri, D. Wibowo, M. Maulidiyah, L. O. A. Salim, T. Azis, C. M. Bijang, F. Mustapa, I. Irwan, Z. Arham and M. Nurdin, *J. Inorg. Organomet. Polym. Mater.*, **31**, 3378 (2021).
20. M. Nurdin, Maulidiyah, A. H. Watoni, N. Abdillah and D. Wibowo, *Int. J. ChemTech Res.*, **9**, 483 (2016).
21. M. Nurdin, A. Zaeni, Maulidiyah, M. Natsir, A. Bampe and D. Wibowo, *Orient. J. Chem.*, **32**, 2713 (2016).
22. N. Tavakkoli, N. Soltani, H. Salavati and M. Talakoub, *J. Taiwan Inst. Chem. Eng.*, **83**, 50 (2018).
23. S. Bakardjieva, J. Šubrt, V. Štengl, M. J. Dianez and M. J. Sayagues, *Appl. Catal. B Environ.*, **58**, 193 (2005).
24. J. Tashkhourian, S. F. N. Ana, S. Hashemnia and M. R. Hormozi-Nezhad, *J. Solid State Electrochem.*, **17**, 157 (2013).
25. P. Srinivasu, S. P. Singh, A. Islam and L. Han, *Adv. Optoelectron.*, **539382**, 1 (2011).
26. A. Yasmin, J. J. Luo and I. M. Daniel, *Compos. Sci. Technol.*, **66**, 1179 (2006).
27. C. Basheer, *J. Chem.*, **456586**, 1 (2013).
28. D. Wibowo, Y. Sufandy, I. Irwan, T. Azis, M. Maulidiyah and M. Nurdin, *J. Mater. Sci. Mater. Electron.*, **28**, 14375 (2020).
29. J. Wang, *Analytical electrochemistry*, John Wiley & Sons (2006).
30. M. Ali Zolfigol and A. G. Choghamarani, *Phosphorus. Sulfur. Silicon Relat. Elem.*, **178**, 1623 (2003).
31. M. Nurdin, T. Azis, M. Maulidiyah, A. Aladin, N. A. Hafid, L. O. A. Salim and D. Wibowo, *IOP Conf. Ser. Mater. Sci. Eng.*, **367**, 012048 (2018).
32. M. Maulidiyah, I. B. P. Wijawan, D. Wibowo, A. Aladin, B. Hamzah and M. Nurdin, *IOP Conf. Ser. Mater. Sci. Eng.*, **367**, 012060 (2018).
33. N. Belkhamsa, L. Ouattara and M. Ksibi, *J. Electrochem. Soc.*, **162**, B212 (2015).
34. P. Bühlmann, E. Pretsch and E. Bakker, *Chem. Rev.*, **98**, 1593 (1998).
35. E. Bakker, P. Bühlmann and E. Pretsch, *Chem. Rev.*, **97**, 3083 (1997).
36. Maulidiyah, D. S. Tribawono, D. Wibowo and M. Nurdin, *Anal. Bioanal. Electrochem.*, **8**, 761 (2016).
37. J. Wang, W. Cui, Q. Liu, Z. Xing, A. M. Asiri and X. Sun, *Adv. Mater.*, **28**, 215 (2016).
38. L. Y. Heng and E. A. H. Hall, *Anal. Chim. Acta*, **443**, 25 (2001).
39. T. Mitsuyama, A. Tsutsumi, T. Hata, K. Ikeue and M. Machida, *Bull. Chem. Soc. Jpn.*, **81**, 401 (2008).
40. L. J. Criscenti and D. A. Sverjensky, *Am. J. Sci.*, **299**, 828 (1999).